EuPA OPEN PROTEOMICS 4 (2014) 25–39

Available online at www.sciencedirect.com

ScienceDirect

journal homepage: http://www.elsevier.com/locate/euprot

Proteomic insights into non-small cell lung cancer: New ideas for cancer diagnosis and therapy from a functional viewpoint

Johannes Linxweiler[a], *Laxmikanth Kollipara*[b], *René P. Zahedi*[b], *Pavel Lampel*[a], *Richard Zimmermann*[a], *Markus Greiner*[a,*]

[a] *Department of Medical Biochemistry and Molecular Biology, Saarland University, Homburg/Saar, Germany*
[b] *Leibniz Institute for Analytical Sciences (ISAS), Dortmund, Germany*

ARTICLE INFO

Article history:
Received 23 October 2013
Received in revised form
18 March 2014
Accepted 21 May 2014
Available online 2 June 2014

Keywords:
Non-small cell lung cancer (NSCLC)
Sec62
2D-DIGE
Vimentin
Plastin 3
Epithelial-mesenchymal transition (EMT)

ABSTRACT

We recently characterized *SEC62* as an oncogene in non-small-cell lung cancer (NSCLC). Here we aimed to gain further insight into the molecular mechanisms of the cancer-related functions of this oncogene. We performed 2D-DIGE proteome analysis of tumor material from patients with NSCLC and of HEK293 cells stably overexpressing plasmid-encoded *SEC62*, combined with investigation of the Sec62 interactome. Furthermore, we analyzed the proteomic effects of siRNA-mediated depletion of the Sec62-interacting protein Sec63. We identified a comprehensive list of differentially regulated proteins, providing new insights into the molecular mechanisms of the cancer-related functions of Sec62 in cell migration, drug resistance, and Ca^{2+}-homeostasis.

1. Introduction

In recent studies, we identified and characterized *SEC62* as a potential new oncogene within the terminal 3q region that is frequently amplified in non-small cell lung cancer (NSCLC) [1]. We further found that *SEC62* gene expression is significantly higher in squamous cell carcinoma (SCC) tumor tissue compared to normal lung tissue, and that Sec62 protein content is significantly elevated in SCC and adenocarcinoma (AC) tumor tissue [1]. In the tissue samples of 70 patients with stage I–III NSCLC, we observed a correlation of Sec62 levels with clinical parameters, including infiltration of the lymph nodes (N^+ vs. N0 tumors) and tumor progression (G3 vs. G2 tumors) [1], and clinical follow-up revealed a significant survival benefit for patients whose tumors exhibited low Sec62 protein content [2].

At the molecular level, Sec62 protein content is apparently responsible for cancer cell migration and invasion [1,3], and for partial protection of cancer cells against thapsigargin-induced endoplasmic reticulum (ER) stress [4]. These phenotypes can be copied to non-cancerous HEK293 cells by

* *Corresponding author*. Tel.: +49 68411626515.
E-mail address: m.greiner@uks.eu (M. Greiner).
http://dx.doi.org/10.1016/j.euprot.2014.05.004

plasmid-driven over-expression of SEC62. We recently also found an influence of Sec62 on cellular calcium homeostasis. First siRNA-mediated Sec62 depletion leads to higher cytosolic calcium concentrations [4], and second plasmid-based overexpression of a *SEC62* gene containing a mutation in a potential EF-hand motif results in the same molecular and cellular phenotypes as seen in Sec62 depletion [2]. Furthermore, a recent systematic gain- and loss-of-function screen in immortalized human mammary epithelial cells found that *SEC62* is a major cancer driver within the 3q26 amplicon [5].

In addition to our research with respect to the cancer-related functions of Sec62, this protein has also been investigated as an accessory component of the protein-conducting Sec61-complex, which can directly interact with ribosomes and thereby regulate translation [6]. Sec62 is also reportedly involved in small protein secretion [7] and post-translational translocation of ppcecA into the ER [8]. Furthermore, regarding the interaction of Sec62 with Sec63, a Hsp40 homologue protein known to directly bind Sec62 was shown to be regulated by CK2-mediated phosphorylation [9]. Despite great progress in understanding the function of Sec62 in protein transport to the ER and in cancer cell biology, the exact molecular mechanisms and signaling pathways behind these functions remain largely unknown.

In our present study, we used the 2D-DIGE technique to search for general proteomic alterations in SCC or AC tumors of the lung versus normal lung tissue. Since the tumor samples were preselected with respect to their Sec62 protein content, we further investigated whether such alterations depended on Sec62 over-production. In cell culture experiments, we specifically over-expressed a plasmid-encoded *SEC62* and then compared the data derived from the different sources. We also present the complimentary results of studying the Sec62 interactome and the consequences of loss of Sec63, the major Sec62 interaction partner.

2. Materials and methods

2.1. *Cell cultures and tissue samples*

The cell lines PC3 (DSMZ no. ACC 465), HEK293 (DSMZ no. ACC 305), and NIH3T3 (DSMC no. ACC 59) were cultured in DMEM medium (Gibco Invitrogen) containing 10% FBS (Biochrom) and 1% penicillin/streptomycin (PAA), at 37 °C in a humidified environment with 5% CO_2. We generated HEK293 cell lines stably transfected with either a plasmid encoding the wild-type *SEC62* gene (p*SEC62*-IRES-GPF) or an empty control plasmid (pIRES-GPF) as previously described [1]. Further cultivation and all experiments using the stably transfected cell lines were performed in normal growth medium containing 1% G418.

Tissue samples were obtained from 70 lung cancer patients with pathologically confirmed AC or SCC. These samples were dissected by a pathologist, sorted into cancerous and healthy portions, snap frozen, and stored at −80 °C. The cancer samples were verified to have >80% tumor cell content by microscopic evaluation of HE-stained cryostat sections. Samples were only used if the patients gave signed informed consent, following the guidelines of the local ethics board.

2.2. *Protein quantification in cultured cells by western blot*

To quantify proteins in the cell culture samples, lysates of 2×10^5 cells per preparation were subjected to western blot analysis using an affinity-purified polyclonal rabbit antibody directed against the carboxy-terminal undecapeptide of human Sec62, a rabbit anti-peptide antiserum directed against CLIMP-63 (PSAKQRGSKGGHC plus CLFVKVEKIHEKV), and an affinity-purified polyclonal rabbit antibody directed against Sec63ΔN380. For loading controls, we also used a polyclonal anti-β-actin (Sigma–Aldrich, A5441-.5ML) or anti-GAPDH antibody (Santa Cruz Biotechnology, FL-335). Vimentin was detected using an anti-Vimentin-Cy3 antibody conjugate (Sigma–Aldrich, C-9080). Bound primary antibodies were visualized with an ECL™ Plex goat-anti-rabbit IgG-Cy5 (GE-Healthcare, PA-45012) or ECL™ Plex goat-anti-mouse IgG-Cy3 conjugate (GE-Healthcare, PA-43010) and the Typhoon-Trio imaging system (GE-Healthcare) with the Image Quant TL software 7.0 (GE-Healthcare). The ratios of Sec62, Sec63, or Vimentin to β-actin or GAPDH were determined.

2.3. *Immunofluorescence staining*

Immunofluorescence double-staining was performed on stably transfected HEK293 cells cultured on glass slides in 6-cm dishes. The cells were washed with PBS, fixed in formaldehyde (3.7% in PBS) at room temperature for 8 min, and permeabilized with 0.2% Triton X-100 and 1% BSA in PBS on ice for 5 min. Then the cells were washed with PBS three times, and non-specific binding sites were blocked by incubation in BSA (1% in PBS). Subsequently, the cells were incubated for 60 min with the above-described specific antibodies against Sec62 or Vimentin-Cy3, or with phalloidin-FITC (Life Technologies, F-432). Sec62 was visualized using a secondary goat-anti-rabbit-FITC antibody conjugate (Dianova, 111-095-144). Cell nuclei were stained with DAPI.

2.4. *Silencing of gene expression by siRNA*

For gene silencing, 5×10^5 NIH3T3 cells were seeded per 6-cm dish in normal culture medium. The cells were transfected with *SEC63* siRNA (GGGAGGUGUAGUUUUUUUAtt, Ambion), *SEC62* siRNA (GGCUGUGGCCAAGUAUCUUtt, Ambion), or control siRNA (AllStars Neg. Control siRNA, Qiagen, 1027281) using HiPerFect Reagent (Qiagen, 301807) following the manufacturer's instructions. After 24, 72, and 144 h, the medium was changed and the cells were transfected again. Silencing efficiency was evaluated by western blot analysis.

2.5. *Proteomic analysis by 2-D difference gel electrophoresis (2D-DIGE)*

HEK293 cells stably overexpressing *SEC62* encoded on a p*SEC62*-IRES-GFP-plasmid, as well as control cells transfected with an empty pIRES-GFP control plasmid, were cultured for 24 h in six independent 25-cm^2 culture flasks. The cells were then trypsinized, harvested, counted, and washed twice with PBS buffer. NIH3T3 cells were cultured and transfected with Sec63 siRNA or control siRNA as described above. At 192 h after

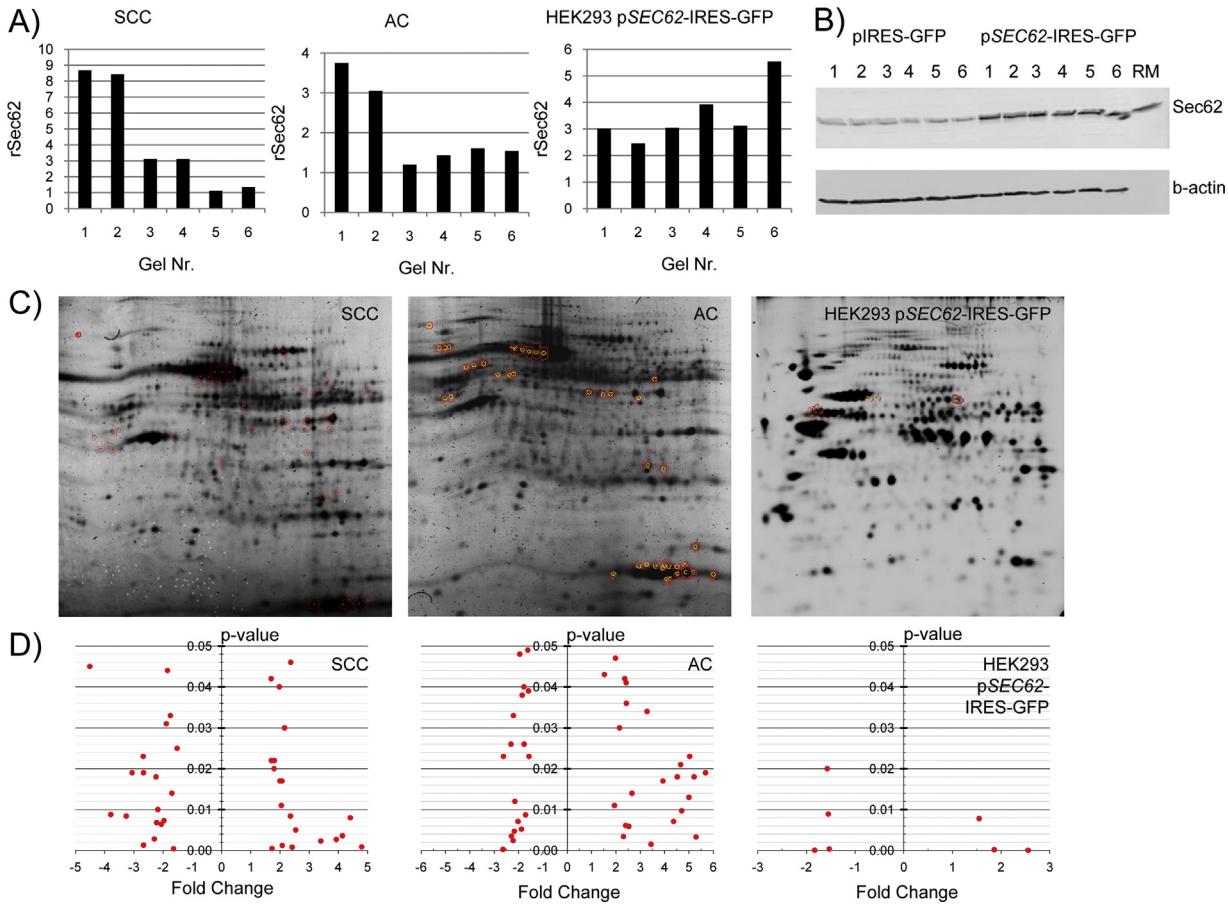

Fig. 1 – Sec62 protein content in samples used for 2D-DIGE. (A) Using western blot analysis, Sec62 and β-actin (loading control) were quantified in all six biological replicates for the SCC and AC patient samples and in the HEK293 samples with either the p*SEC62*-IRES-GFP plasmid or control vector. The Sec62/β-actin ratio was calculated and termed rSec62. (B) Western blot representing the six biological replicates of the *SEC62*-overexpressing (p*SEC62*-IRES-GFP) or non-overexpressing (pIRES-GFP) HEK293-cells that were quantified in (A). (C) The pick-gel from each DIGE-series (SCC, AC and HEK293 p*SEC62*-IRES-GFP) is shown; the picked spots are indicated by a red fringe and the picked areas are indicated by yellow circles. (D) Statistic analysis by DeCyder-software 6.5 for each series of DIGE-gels resulted in the indicated mean fold change ratio and the *p*-value. Here these data for each picked spot are blotted. (For interpretation of the references to color in this figure legend, the reader is referred to the web version of the article.)

the first transfection, the cells were trypsinized, harvested, counted, and washed twice with PBS buffer. Finally the cells from the overexpression and the silencing experiments were lyophilized and stored at −80 °C.

For each experimental approach, 10^6 cells were suspended in 100 μL labeling buffer (7 M Urea, 2 M Thiourea, 65 mM CHAPS, and 25 mM Tris/HCl pH 8.75) and homogenized for 30 s in a MP FastPrep24 homogenizer. Then the proteins were purified using a 2-D Clean-Up kit (Amersham) and quantified using a 2-D Quant kit (Amersham) following the manufacturer's instructions. Tissue samples were snap frozen in liquid nitrogen, and mechanically lysed with a pestle and mortar. Proteins were then isolated using the illustra triplePrep kit (GE Healthcare) following the manufacturer's instructions, and quantified as described.

Six pooled samples were prepared from the tissue of 14 AC or 16 SCC patients by mixing the isolated proteins from two or three patients for each sample. These samples were selected based on their Sec62 protein content as determined by western blot analysis [1], resulting in a mean Sec62 overexpression of 4.2-fold (SCC) or 2.3-fold (AC). From the same patients, matched tumor-free tissue samples were also prepared and pooled in the same manner. The protein extracts were mixed with 0.4 nmol of either Cy3, Cy5, or Cy2 fluorescent dye (GE Healthcare) per 50 μg total protein, and subsequently incubated on ice for 30 min. The reaction was stopped by adding 1 μmol L-lysine. In the DIGE analysis, tumor samples (either SCC or AC) and tumor-free tissue samples were labeled with Cy3 or Cy5 dye, and compared using a Cy2-labeled mixture of both as an internal standard. We used six gels (representing six biological replicates) comparing SCC to normal tissue, and six gels comparing AC to normal tissue. Each gel included dye swaps between tumor and normal tissue to avoid biases by incommensurable labeling reactions.

Finally, the gels were scanned with a Typhoon Trio scanner (GE Healthcare) at a resolution of 100 μm, and protein spots

Table 1 – Proteins that are differently abundant in SCC and AC tumors of the lung compared to normal lung tissue of the same patients.

Spot number[a]	Accession number[b]	Protein name	Molecular mass	emPAI[c]	AV-Ratio[d]	Tumor entity
590	P10809	60 kDa heat shock protein, mitochondrial	61,187	6.3	−2.6	AC
615	P10809	60 kDa heat shock protein, mitochondrial	61,187	19.9	−2.3	AC
630	P10809	60 kDa heat shock protein, mitochondrial	61,187	5.9	−1.6	AC
1479	P05388	60S Acidic ribosomal protein P0	34,423	0.7	1.8	SCC
1613	P18124	60S Ribosomal protein L7	29,264	1.9	4.4	SCC
1642	P18124	60S ribosomal protein L7	29,264	1.6	3.4	SCC
922	P52209	6-Phosphogluconate dehydrogenase, decarboxylating	53,619	0.8	−1.9	SCC
937	P52209	6-Phosphogluconate dehydrogenase, decarboxylating	53,619	0.2	−1.8	SCC
982	P52209	6-Phosphogluconate dehydrogenase, decarboxylating	53,619	0.3	−2.0	SCC
428	P11021	78 kDa glucose-regulated protein	72,402	69.7	−2.3	AC
430	P11021	78 kDa glucose-regulated protein	72,402	17.7	−2.2	AC
442	P11021	78 kDa glucose-regulated protein	72,402	4.9	−1.8	AC
1179	P62736	Actin, aortic smooth muscle	42,381	2.1	2.4	SCC
1314	P62736	Actin, aortic smooth muscle	42,381	1.5	−3.8	SCC
1330	P62736	Actin, aortic smooth muscle	42,381	2.6	−2.7	SCC
1339	P62736	Actin, aortic smooth muscle	42,381	2.9	−2.7	SCC
1179	P60709	Actin, cytoplasmic 1	42,052	2.1	2.4	SCC
1314	P60709	Actin, cytoplasmic 1	42,052	1.3	−3.8	SCC
1330	P60709	Actin, cytoplasmic 1	42,052	2.6	−2.7	SCC
1339	P60709	Actin, cytoplasmic 1	42,052	2.9	−2.7	SCC
1150	P23526	Adenosylhomocysteinase	48,255	2.1	−1.7	SCC
649	Q01518	Adenylyl cyclase-associated protein 1	52,325	2.6	−2.7	SCC
723	P05091	Aldehyde dehydrogenase, mitochondrial	56,859	1.1	−2.0	AC
731	P05091	Aldehyde dehydrogenase, mitochondrial	56,859	1.3	−2.6	AC
175	O43707	Alpha-actinin-4	105,245	0.6	−2.2	SCC
944	P06733	Alpha-enolase	47,481	3.7	−1.9	AC
949	P06733	Alpha-enolase	47,481	1.7	−1.9	AC
975	P06733	Alpha-enolase	47,481	1.1	−1.8	AC
994	P06733	Alpha-enolase	47,481	1.6	−2.2	AC
922	P06733	Alpha-enolase	47,481	13.7	−1.9	SCC
937	P06733	Alpha-enolase	47,481	1.9	−1.8	SCC
982	P06733	Alpha-enolase	47,481	10.2	−2.0	SCC
1019	P06733	Alpha-enolase	47,481	2.6	−1.6	SCC
1168	P06733	Alpha-enolase	47,481	0.5	−3.1	SCC
1192	P06733	Alpha-enolase	47,481	2.6	−3.3	SCC
1518	P07355	Annexin A2	38,808	2.7	1.7	SCC
924	P20073	Annexin A7	52,991	2.2	−1.6	AC
590	P03973	Antileukoproteinase	15,228	0.5	−2.6	AC

– Table 1 (*Continued*)

Spot number[a]	Accession number[b]	Protein name	Molecular mass	emPAI[c]	AV-Ratio[d]	Tumor entity
1117	P13861	cAMP-dependent protein kinase type II-alpha regulatory subunit	45,832	0.2	−2.2	SCC
1626	P00915	Carbonic anhydrase 1	28,909	1.7	2.4	AC
1613	P00915	Carbonic anhydrase 1	28,909	2.7	4.4	SCC
1666	P00918	Carbonic anhydrase 2	29,285	2.6	2.7	AC
1642	P00918	Carbonic anhydrase 2	29,285	1.9	3.4	SCC
605	P04040	Catalase	59,947	1.8	2.0	SCC
539	P07357	Complement component C8 alpha chain	66,832	0.3	2.1	SCC
636	P22528	Cornifin-B	10,337	0.8	2.0	SCC
1019	P31146	Coronin-1A	51,678	0.7	−1.6	SCC
1059	P22695	Cytochrome b-c1 complex subunit 2, mitochondrial	48,584	0.5	−2.2	SCC
631	Q07065	Cytoskeleton-associated protein 4	66,097	3.3	2.4	SCC
979	P81605	Dermcidin	11,391	0.7	−2.0	AC
1626	P81605	Dermcidin	11,391	1.2	2.4	AC
491	Q14195	Dihydropyrimidinase-related protein 3	62,323	0.4	1.5	AC
710	Q99615	DnaJ homolog subfamily C member 7	57,203	2.2	−4.5	SCC
949	P26641	Elongation factor 1-gamma	50,429	3.9	−1.9	AC
1091	P49411	Elongation factor Tu, mitochondrial	49,852	1.8	−2.1	SCC
215	P14625	Endoplasmin	92,696	1.6	−1.7	AC
175	P14625	Endoplasmin	92,696	0.7	−2.2	SCC
2345	Q05315	Eosinophil lysophospholipase	16,556	0.5	5.0	AC
781	Q16658	Fascin	55,123	2.0	−2.2	SCC
711	P02675	Fibrinogen beta chain	56,577	4.8	−1.9	SCC
433	P08107	Heat shock 70 kDa protein 1A/1B	70,294	2.4	2.2	AC
437	P08107	Heat shock 70 kDa protein 1A/1B	70,294	9.3	2.3	AC
461	P08107	Heat shock 70 kDa protein 1A/1B	70,294	2.1	2.4	AC
482	P08107	Heat shock 70 kDa protein 1A/1B	70,294	0.7	2.0	AC
488	P02790	Hemopexin	52,385	0.5	1.9	AC
484	P02790	Hemopexin	52,385	0.4	2.4	SCC
515	P02790	Hemopexin	52,385	0.4	2.1	SCC
615	P61978	Heterogeneous nuclear ribonucleoprotein K	51,230	2.9	−2.3	AC
630	P61978	Heterogeneous nuclear ribonucleoprotein K	51,230	1.1	−1.6	AC
605	P14866	Heterogeneous nuclear ribonucleoprotein L	64,720	0.8	2.0	SCC
2234	Q71DI3	Histone H3.2	15,436	1.2	−1.6	AC
2339	P62805	Histone H4	11,360	1.2	5.2	AC
2360	P62805	Histone H4	11,360	0.7	5.0	AC

– Table 1 (*Continued*)

Spot number[a]	Accession number[b]	Protein name	Molecular mass	emPAI[c]	AV-Ratio[d]	Tumor entity
2363	P62805	Histone H4	11,360	0.7	4.7	AC
2364	P62805	Histone H4	11,360	2.8	4.5	AC
2423	P62805	Histone H4	11,360	2.8	4.7	AC
2434	P62805	Histone H4	11,360	0.7	3.4	AC
2441	P62805	Histone H4	11,360	2.8	3.9	AC
2501	P62805	Histone H4	11,360	1.9	2.4	AC
2243	P62805	Histone H4	11,360	1.9	5.2	SCC
491	P01876	Ig alpha-1 chain C region	38,486	0.4	1.5	AC
484	P01876	Ig alpha-1 chain C region	38,486	0.3	2.4	SCC
599	P01876	Ig alpha-1 chain C region	38,486	0.9	1.8	SCC
610	P01876	Ig alpha-1 chain C region	38,486	0.9	2.2	SCC
643	P01876	Ig alpha-1 chain C region	38,486	0.9	2.5	SCC
730	P01857	Ig gamma-1 chain C region	36,596	1.2	−2.2	AC
731	P01857	Ig gamma-1 chain C region	36,596	1.2	−2.6	AC
730	P01859	Ig gamma-2 chain C region	36,505	0.8	−2.2	AC
908	P01861	Ig gamma-4 chain C region	36,431	0.8	1.7	SCC
723	P01764	Ig heavy chain V-III region VH26	12,745	1.0	−2.0	AC
716	P01834	Ig kappa chain C region	11,773	1.8	2.1	SCC
369	P01871	Ig mu chain C region	49,960	1.2	1.7	SCC
1479	P50213	Isocitrate dehydrogenase [NAD] subunit alpha, mitochondrial	40,022	0.6	1.8	SCC
1518	P50213	Isocitrate dehydrogenase [NAD] subunit alpha, mitochondrial	40,022	2.0	1.7	SCC
994	O75874	Isocitrate dehydrogenase [NADP] cytoplasmic	46,915	0.6	−2.2	AC
1091	O75874	Isocitrate dehydrogenase [NADP] cytoplasmic	46,915	2.2	−2.1	SCC
461	Q03252	Lamin-B2	67,762	0.9	2.4	AC
482	Q03252	Lamin-B2	67,762	1.4	2.0	AC
488	Q03252	Lamin-B2	67,762	0.5	1.9	AC
599	Q03252	Lamin-B2	67,762	3.1	1.8	SCC
515	P09960	Leukotriene A-4 hydrolase	69,868	0.4	2.1	SCC
539	P09960	Leukotriene A-4 hydrolase	69,868	0.6	2.1	SCC
711	Q9HCC0	Methylcrotonoyl-CoA carboxylase beta chain, mitochondrial	61,808	2.9	−1.9	SCC
1275	O43684	Mitotic checkpoint protein BUB3	37,587	1.1	−1.5	SCC
215	P59665	Neutrophil defensin 1	10,536	0.8	−1.7	AC
1275	P59665	Neutrophil defensin 1	10,536	0.8	−1.5	SCC
781	P43490	Nicotinamide phosphoribosyltransferase	55,772	4.0	−2.2	AC
2234	P62937	Peptidyl-prolyl cis-trans isomerase A	18,229	14.2	−1.6	AC
1059	P00558	Phosphoglycerate kinase 1	44,985	1.2	−2.2	SCC
437	P13797	Plastin-3	71,279	1.1	2.3	AC
636	P13797	Plastin-3	71,279	1.8	2.0	SCC
610	P02545	Prelamin-A/C	74,380	3.5	2.2	SCC
631	P02545	Prelamin-A/C	74,380	1.5	2.4	SCC
643	P02545	Prelamin-A/C	74,380	1.0	2.5	SCC

– Table 1 (*Continued*)

Spot number[a]	Accession number[b]	Protein name	Molecular mass	emPAI[c]	AV-Ratio[d]	Tumor entity
1150	Q9UQ80	Proliferation-associated protein 2G4	44,101	1.8	−1.7	SCC
716	O15460	Prolyl 4-hydroxylase subunit alpha-2	61,263	1.4	2.1	SCC
2243	P05109	Protein S100-A8	10,885	2.0	5.2	SCC
710	P14618	Pyruvate kinase isozymes M1/M2	58,470	0.9	−4.5	SCC
924	P50395	Rab GDP dissociation inhibitor beta	51,087	9.1	−1.6	AC
944	P50395	Rab GDP dissociation inhibitor beta	51,087	1.3	−1.9	AC
908	Q13228	Selenium-binding protein 1	52,928	0.9	1.7	SCC
369	P02787	Serotransferrin	79,294	20.8	1.7	SCC
433	P38646	Stress-70 protein, mitochondrial	73,920	4.2	2.2	AC
649	Q99832	T-complex protein 1 subunit eta	59,842	3.5	−2.7	SCC
428	P40939	Trifunctional enzyme subunit alpha, mitochondrial	83,688	1.0	−2.3	AC
430	P40939	Trifunctional enzyme subunit alpha, mitochondrial	83,688	0.5	−2.2	AC
442	P40939	Trifunctional enzyme subunit alpha, mitochondrial	83,688	0.8	−1.8	AC
975	P08670	Vimentin	53,676	49.8	−1.8	AC
979	P08670	Vimentin	53,676	23.9	−2.0	AC
1117	P08670	Vimentin	53,676	2.9	−2.2	SCC
1168	P08670	Vimentin	53,676	0.9	−3.1	SCC
1192	P08670	Vimentin	53,676	1.3	−3.3	SCC

[a] The number given by the software DeCyder (GE-Healthcare).
[b] From the UniProt KD database (http://www.uniprot.org).
[c] The exponentially modified protein abundance index in the respective spot [10].
[d] An *n*-fold regulation of the spot; a negative value stands for an up-regulation in the tumor, a positive value for a down-regulation.

were detected with the DeCyder software (GE-Healthcare, version 6.5) with the target spot number set to 2000. For further analysis, we selected spots meeting the following criteria: presence in at least five out of six biological replicates (SCC samples and cell cultures) or in four out of five biological replicates (AC samples); statistically significant regulation in all replicates, with a p value < 0.05; relative regulation of at least 1.5-fold (higher or lower). All regulated spots matching these criteria were picked from the gel and analyzed by nano-LC-MS/MS. The resulting peptide sequences were assigned to proteins based on a database search (IPI human database, EBI), and their emPAI-values [10] were calculated. From the list of regulated proteins in the tissue samples, keratins and hemoglobin subunits were dismissed. For all 2D-DIGE analyses, the proteins identified in each spot were arranged by the emPAI-value and the two top listed proteins were selected for the tables, which are presented here. The original data are shown in the Supplement.

2.6. *Co-immunoprecipitation*

For co-immunoprecipitation, 6×10^8 HEK293 cells stably transfected with the p*SEC62*-IRES-GFP plasmid were harvested, suspended in 64 mL lysis buffer containing 20 mM HEPES/KOH pH 7.55, 1.5 mM $MgCl_2$, 1 mM EDTA, 150 mM KCl, 0.65% CHAPS, and protease inhibitor (12 μg/mL each pepstatin A, leupeptin, antipain, chrymostatin, and 200 μM phenylmethylsulfonylfluoride). These cells were incubated for 1.5 h at 4 °C for cell lysis, and centrifuged at 257,000 × *g* for 20 min at 2 °C. Next, two 22.5 mL aliquots of the supernatant were incubated overnight at 4 °C: one with 0.5 mg of an affinity-purified polyclonal rabbit anti-peptide antibody directed against the COOH terminus of human Sec62, and the other with 0.5 mg of an affinity-purified polyclonal rabbit antibody directed against GST. Each antibody was pre-bound to protein A/G sepharose mix (Fastflow, GE Healthcare, 1:1). The suspension was subsequently transferred into a column (Mobi-Tec). After collecting the

Table 2 – Differently abundant proteins in HEK293 p*SEC62*-IRES-*GFP* cells compared to HEK293 pIRES-*GFP* cells.

Spot number[a]	Accession number[b]	Protein name	Molecular mass	emPAI[c]	AV ratio[d]
1389	P10809	60 kDa heat shock protein, mitochondrial	61,187	1.85	−1.55
1448	P10809	60 kDa heat shock protein, mitochondrial	61,187	30.7	−1.53
1457	P10809	60 kDa heat shock protein, mitochondrial	61,187	8.02	−1.83
1325	P31939	Bifunctional purine biosynthesis protein PURH	65,089	4.61	1.55
1258	P08107	Heat shock 70 kDa protein 1A/1B	70,294	9.75	1.86
1259	P08107	Heat shock 70 kDa protein 1A/1B	70,294	1.49	2.56
1258	P13797	Plastin-3	71,279	2.53	1.86
1259	P13797	Plastin-3	71,279	1.82	2.56
1473	P30153	Serine/threonine-protein phosphatase 2A 65 kDa regulatory subunit A alpha isoform	66,065	4.21	−1.57
1325	P31948	Stress-induced-phosphoprotein 1	63,227	14.41	1.55
1389	P08670	Vimentin	53,676	34.51	−1.55
1448	P08670	Vimentin	53,676	176.02	−1.53
1457	P08670	Vimentin	53,676	80.68	−1.83
1473	P08670	Vimentin	53,676	3.98	−1.57

[a] The number given by the software DeCyder (GE-Healthcare).
[b] From the UniProt KD database (http://www.uniprot.org).
[c] The exponentially modified protein abundance index in the respective spot [10].
[d] An *n*-fold regulation of the spot; a negative value stands for an up-regulation in the tumor, a positive value for a down-regulation.

flow-through, the column was washed three times with the lysis buffer, and another three times with a washing buffer containing 50 mM Tris/HCl pH 7.4, 150 mM NaCl, 5 mM EDTA, 0.5% Nonidet P40, and the above-described protease inhibitor. Eight 500-μL fractions of the bound material were eluted from the columns using washing buffer supplemented with 1 mg/mL of the peptide against which the anti-Sec62 antibody was directed to. The eluted proteins were precipitated following the method described by Wessel [11], and then loaded on a SDS gel and stained with Coomassie brilliant blue. Protein bands were subsequently analyzed by nano-LC–MS/MS. The determined peptide sequences were assigned to proteins based on a database search (IPI human database, EBI), and emPAI-values [10] were calculated for each protein result. Proteins identified for each band were arranged by emPAI-values and the three top listed proteins were selected for the tables, which are presented here. Here also the molecular mass of the denatured protein was taken into consideration. The original data are shown in the Supplement.

3. Results and discussion

3.1. *Proteomic comparison of tumor and normal tissue of the lung*

In our first approach, we investigated the proteomic alterations in tumor samples derived from SCC or AC of the lung, which were compared to tumor-free lung tissue from the same patients. We analyzed paired fresh-frozen tissue samples from a total of 30 patients suffering from stage II or IIIA NSCLC (16 SCC and 14 AC) and undergoing surgical resection with a curative intention. This large number of patients allowed us to obtain statistically reliable data for each NSCLC subtype individually. In lung cancer, the genomic region 3q25-26 where the *SEC62* gene is located has been shown to be more frequently amplified in squamous cell carcinoma (55–85%) compared to adenocarcinoma (25–30%) [12,13]. Here we pooled the samples according to their previously determined Sec62 protein content [1], creating six biological replicates, each including tissue samples from two to four cases. The relative Sec62 protein content in each pooled sample was again determined by western blot (Fig. 1).

Using the 2D-DIGE approach for the SCC samples, we found 73 spots representing 49 different proteins that were significantly regulated in tumor compared to tumor-free lung tissue (relative protein abundance of 1.5-fold higher or lower) and detected in at least 5 of 6 replicates. Of these proteins, 24 were up-regulated and 25 were down-regulated. In the AC samples, we detected 59 spots representing 32 proteins meeting the afore-mentioned criterion for relative regulation and being present in at least 4 of 5 replicates. Of these proteins, 20 were up-regulated and 11 down-regulated. Eleven proteins were found to be significantly regulated in both SCC and AC tissue; five of the latter were up-regulated and six down-regulated, and in all cases, the observed regulation tended toward the same direction in both analyzed histological entities. Table 1 presents a detailed list of all identified proteins.

The protein dermcidin was found to be regulated in two spots in AC tissue, but the direction of regulation remained unclear, as one spot showed down-regulation (2.4-fold) while the other showed up-regulation (2.0-fold). This phenomenon might result from the post-translational modification that has been described for this protein, or from limited proteolysis leading to several truncated peptides [14,15]. This 110 amino-acid secretory protein almost meets the criteria for small

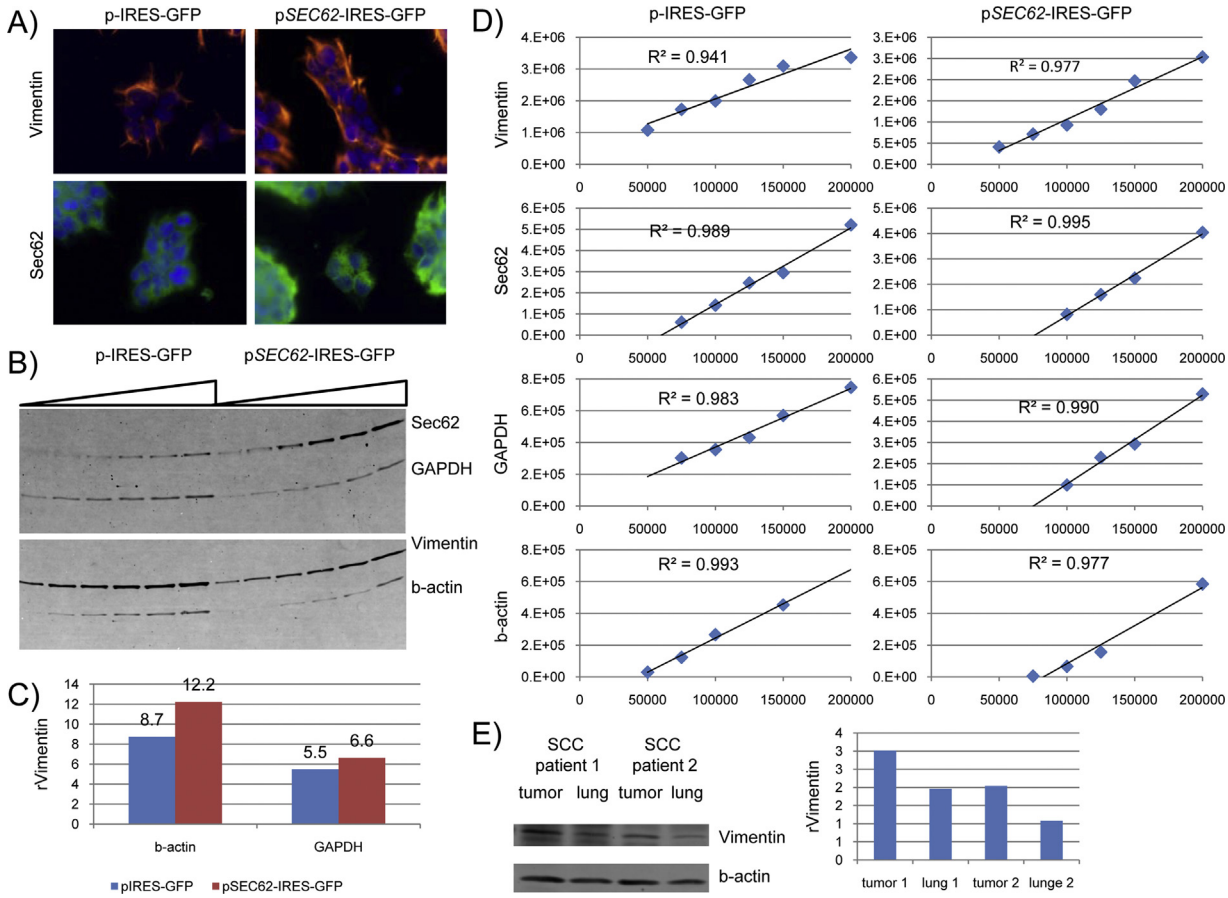

Fig. 2 – Regulation of the Vimentin protein content and localization with and without *SEC62* overexpression. (A) Sec62 and Vimentin were analyzed in HEK293 cells with *SEC62* overexpression (p*SEC62*-IRES-GFP) and without (p-IRES-GFP), using a Cy3-coupled antibody directed against Vimentin and a rabbit anti-Sec62 antibody combined with a FITC-coupled anti-rabbit antibody. (B) Sec62 and Vimentin protein levels in HEK293 cells were quantified by western blot analysis. (C) The amounts of Sec62, Vimentin, and β-actin or GAPDH (loading control) were quantified at different cell numbers (50,000, 75,000, 100,000, 125,000, 150,000, and 200,000 cells per lane), and the ratio of Sec62 or Vimentin to β-actin and GAPDH was calculated. The mean values of these ratios were compared between Sec62-overproducing (p*SEC62*-IRES-GFP) and non-overproducing (pIRES-GFP) cells. (D) The linearity of the signal intensity was proofed for all proteins. (E) Vimentin and β-actin protein contents were quantified by western blot analysis of tumor tissue and normal lung tissue of two different SCC tumor patients, and the ratio of Vimentin to β-actin was calculated (rVimentin).

proteins that strongly depend on Sec62 for efficient translocation to the ER [7]. It also contains a large disordered region within its N-terminal sequence [15], which might affect its translocation to the ER [16]. Therefore, the accumulation of modified or partially digested dermcidin derivates might be due to the influence of Sec62 on its translocation to the ER.

Among the regulated proteins, we also found an enrichment of proteins involved in ER-stress response, such as endoplasmin and BiP. Two previous studies using 2D-DIGE technology show that BiP is differentially abundant in thyroid cancer [17,18], and another important study demonstrates a crucial function of BiP in angiogenesis, and describes this protein as an effective target molecule for cancer anti-neovascular therapy [19]. Our present results also identified proteins with known functions in cell migration and invasion, such as hemopexin and Hsp70 1A/1B, and cytoskeleton-associated proteins, such as Vimentin, fascin, and cytoskeleton-associated protein 4 (CLIMP-63). Within these proteins CLIMP-63 is of special interest as this protein is normally controlling the ER-shape and the anchoring of microtubules to the ER in a phosphorylation and cell-cycle dependent manner [20]. Studies investigating the effect of synthetic inhibitors (olomoucine, roscovitine) of cyclin-dependent kinases (CDK) on cancer cell proliferation and p53 protein content in human cancer cells unexpectedly found an increase of CLIMP-63 after olomoucine-treatment [21,22]. Taken together, these results perfectly support our previous findings that *SEC62*-overexpressing tumors have a higher invasion potential and are protected against thapsigargin-induced ER stress [1,3,4], as well as identify new and previously known proteins that are regulated in cancer.

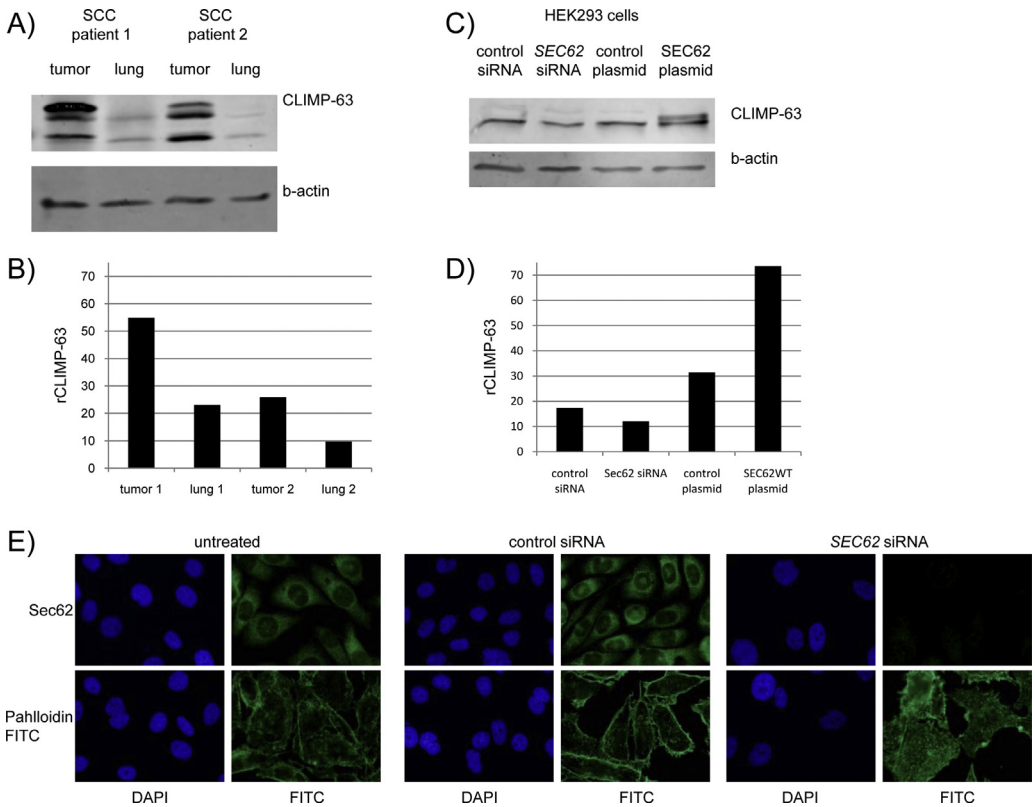

Fig. 3 – Sec62-dependent regulation of CLIMP-63 in SCC tumor samples and HEK293 cells. (A) The amounts of CLIMP-63 and β-actin (loading control) were analyzed by western blot analysis of tumor tissue and normal lung tissue from two different SCC tumor patients. (B) The signal intensity from (A) was quantified, and the ratio of CLIMP-63 to β-actin was calculated (rCLIMP-63). (C) Sec62 and Vimentin protein levels were quantified by western blot analysis of HEK293 cells either after Sec62 depletion by siRNA treatment compared to control siRNA transfected cells, or after SEC62 over-expression. (D) The signal intensity from (C) was quantified, and the ratio of CLIMP-63 to β-actin was calculated (rCLIMP-63). (E) The Sec62 protein content and the cellular localization of f-actin are shown by immunofluorescence staining using a rabbit anti-Sec62 antibody combined with a FITC-coupled anti-rabbit antibody and a phalloidin-FITC conjugate. Cell nuclei were stained with DAPI.

3.2. *Specific alterations in the proteome of HEK293 cells induced by SEC62 overexpression*

Next, we analyzed proteomic differences between HEK293 cells stably overexpressing a plasmid-encoded *SEC62* gene (pcDNA3-*SEC62*-IRES-*GFP*) and control cells transfected with an empty–vector plasmid (pcDNA3-IRES-*GFP*). We used a non-tumor-originated cell line in order to focus specifically on proteomic alterations caused by the increased amount of Sec62 protein. Within the six biological replicates used in 2D-DIGE experiments, the relative Sec62 protein levels in the *SEC62*-overexpressing cells ranged from 246 to 554% (Fig. 1). As expected, we detected much fewer proteomic alterations as compared to our analysis of tumor material. Table 2 shows that we found only three spots (1258, 1259, and 1457) to be consistently regulated in all six biological replicates. Among these, we again identified Hsp70 1A/1B (1258 and 1259), which is described in the literature as having anti-apoptotic and carcinogenic effects [23] and as being a driving force for cancer cell migration and invasion [24,25]. We also identified plastin 3 (1258 and 1259), an actin-binding protein harboring a potential calcium-binding site in its N-terminus, which was previously described as being down-regulated in A549 lung cancer cells after apoptosis induction [26]. Finally, we found Vimentin (1457), a well-established marker for epithelial-mesenchymal transition (EMT) [27], which is known to be up-regulated in many cancer entities-including lung cancer, where it is associated with an unfavorable prognosis [27] and also considered as a "druggable" molecular target [28]. When including spots regulated in at least five of the six biological replicates, three more could be selected (1389, 1448, and 1473). All of these again represented Vimentin (1389 and 1448), and were regulated in the same direction as spot 1457. The third spot (1473) also contained serine/threonine-protein phosphatase 2A regulatory subunit Aα, PP2A Aα. This was a very interesting finding, because the interaction of Sec62 with Sec63 (a known binding partner of Sec62 in the ER membrane) was previously shown to depend on the phosphorylation status of Sec63, which is phosphorylated by CK2 [9]-and PP2A is a long-known antagonist of CK2 [29]. Additionally, PP2A mutations reportedly increase the incidence of lung cancer in mice [30]. In three of our six biological replicates, we identified the stress-induced phosphoprotein 1 (Hop1 or STIP1, spot 1325), which also reportedly plays a role in carcinogenesis [31]

Table 3 – Proteins that co-precipitated with Sec62 from HEK293 p*SEC62*-IRES-*GFP* cells.

Band number[a]	Accession number[b]	Protein name	Molecular mass	emPAI
4	Q92616	Translational activator GCN1	294,967	0.54
6	P49815	Tuberin	202,591	0.07
8	P49815	Tuberin	202,591	0.12
10	P49815	Tuberin	202,591	0.1
12	Q8IX12	Cell division cycle and apoptosis regulator protein 1	133,423	1.7
14	Q8IUD2	ELKS/Rab6-interacting/CAST family member 1	128,236	0.7
16	Q8IX12	Cell division cycle and apoptosis regulator protein 1	133,423	1.28
18	Q14566	DNA replication licensing factor MCM6	93,801	0.62
20	Q13033	Striatin-3	87,554	0.25
22	P13639	Elongation factor 2	96,246	0.65
24	P08238	Heat shock protein HSP 90-beta	83,554	0.85
26	O95202	LETM1 and EF-hand domain-containing protein 1, mitochondrial	83,986	0.64
28	P11142	Heat shock cognate 71 kDa protein	71,082	1.06
30	P08107	Heat shock 70 kDa protein 1A/1B	70,294	2.76
34	Q9H078	Caseinolytic peptidase B protein homolog	79,193	0.63
36	P08670	Vimentin	53,676	9.18
38	Q99442	Translocation protein SEC62	46,175	3.26
40	Q5VTE0	Putative elongation factor 1-alpha-like 3	50,495	1.14
42	P60709	Actin, cytoplasmic 1	42,052	2.9
44	Q96HS1	Serine/threonine-protein phosphatase PGAM5, mitochondrial	32,213	0.48
46	P81605	Dermcidin	11,391	0.69
48	P04075	Fructose-bisphosphate aldolase A	39,851	0.38
50	P35232	Prohibitin	29,843	0.37
52	O75323	Protein NipSnap homolog 2	33,949	0.32
54	O75323	Protein NipSnap homolog 2	33,949	0.32

[a] The number shown in Fig. 4.
[b] Refers to the UniProt KD database (www.uniprot.org).

and is considered a prognostic biomarker in ovarian cancer [32].

Interestingly, the proteins Hsp70 1A/1B, Vimentin, and plastin 3 were identified as regulated in AC and/or SCC tumor tissue as well as in *SEC62*-overexpressing HEK293 cells, with the regulation tending toward the same direction in all cases. Hence, for these proteins, we suggest that the observed regulation is Sec62 dependent. To verify this assumption, we also examined the Vimentin protein content of the HEK293 cell lines used for 2D-DIGE analysis via western blot analysis and indirect immunofluorescence. Analyzing *SEC62*-overexpressing and non-overexpressing HEK293 cells with this technique, we found slightly increased Vimentin signal intensity in the former (Fig. 2A). Western blot experiments revealed a 1.2- to 1.4-fold increase of the Vimentin protein content in HEK293 cells harboring the wild-type *SEC62* encoding plasmid compared to the empty vector control (Fig. 2B). As these values were on the borderline of western blot accuracy, we carefully evaluated the signal linearity for Vimentin, β-actin, and GAPDH (Fig. 2D). The detection of Vimentin in tumor samples confirmed the increased Vimentin protein content in tumor compared to normal lung tissue (Fig. 2E).

The same was true for CLIMP-63, a second cytoskeleton-associated protein that exhibited differential abundance in our SCC tumor sample approach but not in the DIGE analysis using the HEK293-cells. We detected a strongly increased signal in the SCC tumor samples, but hardly any signal in normal lung tissue (Fig. 3A and C). To analyze whether this regulation really depended on the Sec62 protein level, we studied the CLIMP-63 protein content in HEK293 cells treated with

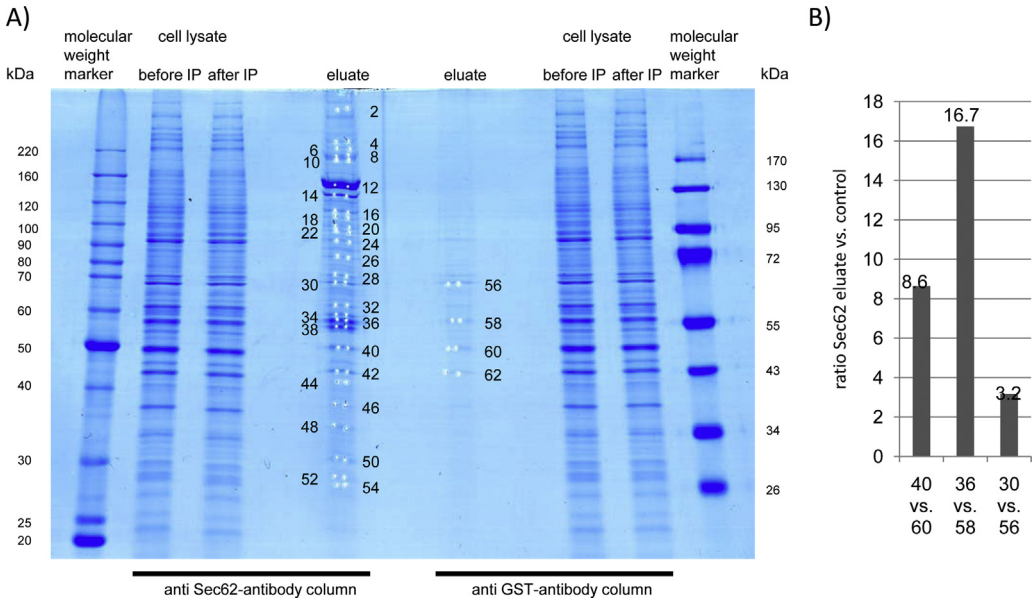

Fig. 4 – Co-immunoprecipitation of Sec62-interacting proteins. HEK293 cells stably transfected with the pSEC62-IRES-GFP plasmid were harvested, lysed, and the supernatant was incubated with an affinity-purified polyclonal rabbit anti-peptide antibody directed against the COOH terminus of human Sec62 or GST. The suspension was subsequently transferred into a column, washed, and eluted using washing buffer supplemented with 1 mg/mL of the peptide against which the anti-Sec62 antibody was directed. The eluted protein was precipitated following the method described by Wessel [11], loaded on a SDS gel, and stained with Coomassie brilliant blue. Proteins analyzed in 56–62 are included in the respective supplemental file.

SEC62 siRNA or control siRNA, and we found reduced CLIMP-63 protein content after Sec62 depletion. Furthermore, overexpression of *SEC62* led to increased CLIMP-63 protein content. These cells exhibited a second band with an increased molecular weight, potentially indicating a post-translational modification (Fig. 3B and D). CLIMP-63 is regulated by phosphorylation during the cell cycle [20].

Thus, overproduction of Vimentin and CLIMP-63 indeed depended on *SEC62* overexpression in HEK293 cells. To directly study the influence of Sec62 on the actin rearrangement indicated by the regulation of this set of actin-interacting proteins, we stained f-actin with a phalloidin-FITC conjugate in PC3 cells that were either untreated or transfected with control siRNA or *SEC62* siRNA. Our results revealed a rearrangement of the f-actin from being localized rather near the plasma membrane in the presence of Sec62, to being equally distributed throughout the cell after Sec62 depletion (Fig. 3E). Thus, changes in calcium-induced actin rearrangement in the absence of Sec62 might contribute to the strongly reduced migration potential of these cells.

3.3. *From the proteomic view to the interactome of Sec62*

In addition to the alterations in tumor tissue and in *SEC62*-overexpressing cultured cells, we also studied the Sec62 interactome in HEK293 cells stably overexpressing the plasmid-encoded *SEC62* gene. To this end, we performed co-immunoprecipitation experiments using an affinity-purified antibody directed against the COOH-terminal undecapeptide of Sec62 that was previously shown to be highly specific under native and denaturing conditions [3]. Table 3 summarizes all proteins that co-precipitated with Sec62, and Fig. 4 shows the respective Coomassie-stained SDS gel. Our results showed two Sec62-interacting proteins, Hsp70 1A/1B and Vimentin, both of which had previously shown a differential abundance in at least one of the tumor tissue samples and in the *SEC62*-overexpressing HEK293 cells. The co-immunoprecipitation results also showed several other proteins with functions related to the cancer phenotypes induced by *SEC62* overexpression, including the cell division cycle and apoptosis regulator protein 1 (CCAR1), which is described as a key regulator of apoptosis signaling [33], and the ELKS/Rab6 interacting protein (ERC-1), which is reportedly involved in the development of papillary thyroid carcinoma [34].

Another highly interesting interaction partner of Sec62-especially with respect to its regulatory function in ER calcium homeostasis [2]-is striatin-3, a calmodulin binding [35] and PP2A-interacting protein [36–38]. Sec62 interacted with LETM1, which, like Sec62 itself, is an EF-hand-containing calcium-binding protein; however, due to its location in the inner mitochondrial membrane [39], it is unlikely that its interaction with Sec62 is physiologically relevant. Prohibitin, which was also found to interact with Sec62 in this assay, is also located in the mitochondria but can be found in the plasma membrane as well [40], making it a possible substrate for Sec62-dependent membrane insertion. Prohibitin is also linked to cancer-related functions, such as androgen receptor signaling [41] and regulation of cell proliferation [42] and apoptosis [43]. We also analyzed four bands, picked from the eluate of the GST-antibody-column. In three of these bands we found Hsp70 1A/1B, Vimentin and the putative elongation factor 1-alpha-like 3, i.e., the same proteins as compared to the Sec62-antibody-column. However, quantification showed

much less interaction in the control (Fig. 4B) and so also these candidates bound specific to Sec62. In summary, this approach revealed several intersections of the Sec62 interactome with the regulated proteins identified in the 2D-DIGE experiments, as well as highlighted several interesting candidate proteins in the context of cancer development, disease progression, or metastasis.

3.4. *Depletion of Sec63 leads to overlapping proteomic changes*

Next, we investigated the influence of Sec63 depletion on the cellular proteome, as this protein is a known interaction partner of Sec62 [9,44,45] and likewise part of the protein translocation machinery in the ER membrane. Furthermore, the *SEC63* gene is among the most frequently mutated genes in hereditary nonpolyposis colorectal cancer-associated small-bowel cancer, and in sporadic cancers with frequent microsatellite instability [46,47]. Here we depleted the Sec63 protein in NIH3T3 cells by repeated transfection with siRNA, evaluated the silencing efficiency by western-blot (supplementary Fig. S1A), and subsequently used the lysates of six independent experiments for 2D-DIGE analysis. Interestingly, we found only four spots to be regulated by more than 1.5-fold (*t*-test: $p < 0.5$, appearance in more than 12 spot maps), representing four different proteins: cytoskeleton associated protein 4 (CLIMP-63), tyrosyl tRNA-synthetase, WD repeat-containing protein 1, and prelamin A/C (supplementary Table S1 and Fig. S1B). Two of the proteins (CLIMP-63 and prelamin A/C) that were significantly up-regulated upon Sec63 depletion were also found to be up-regulated in the Sec62-overproducing SCC samples as compared to adjacent tumor-free lung tissue. Thus, it appears that these opposite changes in the Sec62 or Sec63 protein content both lead to the same effect: up-regulation. As CLIMP-63 is an integral ER-membrane protein [20,48] that influences the mobility of ER translocon complexes through its interaction with microtubules [49], one might speculate that Sec62/Sec63 functions in regulating its membrane insertion.

4. Conclusions

Proteomic studies represent a powerful tool for investigating the biological background of a disease on the molecular level, and thus providing the detailed mechanistic insights necessary for developing new therapeutic strategies. To overcome the individual disadvantages of single experimental approaches, here we studied the proteomes of different *SEC62* overexpressing tumor types, including SCC and AC of the lung, and of a more defined cell culture system specifically overexpressing *SEC62*. We investigated *SEC62* overexpression because we previously characterized it as a new candidate oncogene [1] and it has been characterized as a cancer driver gene in NSCLC by others [5]. The results of the present study provide new insights into the complex molecular background of the tumor-related functions of Sec62. We identified three proteins regulated in SCC and/or AC as well as in the *SEC62*-overexpressing HEK293 cells-namely, HSP70 1A/B, plastin-3, and Vimentin. Of these, HSP70 1A/B and

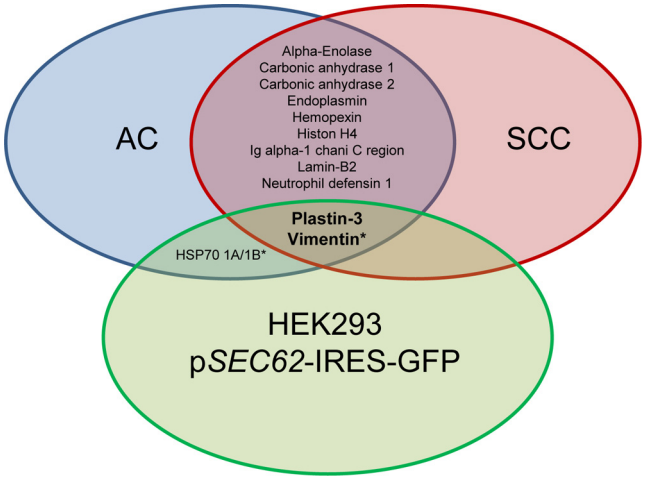

Fig. 5 – Overlapping results of different proteome studies. The proteins found in at least two proteome studies are shown in a Venn diagram. Proteins marked with an asterisk also co-immunoprecipitated with Sec62.

Vimentin also co-immunoprecipitated with Sec62, indicating a direct protein–protein interaction (Fig. 5). We suggest that one or more of the observed cytoskeletal effects of SEC62 overexpression, together with altered calcium homeostasis, contribute to the hallmarks of SEC62-overexpressing (tumor) cells, i.e., increased migration potential and increased ER stress tolerance.

Financial support

Grant from the Deutsche Forschungsgemeinschaft FOR967 (R. Zimmermann), grant from the "Freunde des Universitätsklinikums des Saarlandes" (J. Linxweiler).

Conflicts of interest

We have no assumed or potential conflict of interest to disclose.

Appendix A. Supplementary data

Supplementary data associated with this article can be found, in the online version, at doi:10.1016/j.euprot.2014.05.004.

REFERENCES

[1] Linxweiler M, Linxweiler J, Barth M, Benedix J, Jung V, Kim YJ, et al. Sec62 bridges the gap from 3q amplification to molecular cell biology in non-small cell lung cancer. Am J Pathol 2012;180:473–83.
[2] Linxweiler M, Schorr S, Schäuble N, Jung M, Linxweiler J, Langer F, et al. Targeting cell migration and the endoplasmic reticulum stress response with calmodulin antagonists: a clinically tested small molecule phenocopy of SEC62 gene silencing in human tumor cells. BMC Cancer 2013;13:574–87.

[3] Greiner M, Kreutzer B, Jung V, Grobholz R, Hasenfus A, Stöhr RF, et al. Silencing of the SEC62 gene inhibits migratory and invasive potential of various tumor cells. Int J Cancer/J Int Du Cancer 2011;128:2284–95.
[4] Greiner M, Kreutzer B, Lang S, Jung V, Adolpho C, Unteregger G, et al. Sec62 protein content is crucial for the ER stress tolerance of prostate cancer. Prostate 2011;71:1074–83.
[5] Hagerstrand D, Tong A, Schumacher SE, Ilic N, Shen RR, Cheung HW, et al. Systematic interrogation of 3q26 identifies TLOC1 and SKIL as cancer drivers. Cancer Discov 2013;3:1044–57.
[6] Muller L, Diaz de Escauriaza M, Lajoie P, Theis M, Jung M, Muller A, et al. Evolutionary gain of function for the ER membrane protein Sec62 from yeast to humans. Mol Biol Cell 2010;21:691–703.
[7] Lakkaraju AK, Thankappan R, Mary C, Garrison JL, Taunton J, Strub K. Efficient secretion of small proteins in mammalian cells relies on Sec62-dependent posttranslational translocation. Mol Biol Cell 2012;23:2712–22.
[8] Lang S, Benedix J, Fedeles SV, Schorr S, Schirra C, Schauble N, et al. Different effects of Sec61alpha, Sec62 and Sec63 depletion on transport of polypeptides into the endoplasmic reticulum of mammalian cells. J Cell Sci 2012;125:1958–69.
[9] Ampofo E, Welker S, Jung M, Muller L, Greiner M, Zimmermann R, et al. CK2 phosphorylation of human Sec63 regulates its interaction with Sec62. Biochim Biophys Acta 2013;1830:2938–45.
[10] Ishihama Y, Oda Y, Tabata T, Sato T, Nagasu T, Rappsilber J, et al. Exponentially modified protein abundance index (emPAI) for estimation of absolute protein amount in proteomics by the number of sequenced peptides per protein. Mol Cell Proteom 2005;4:1265–72.
[11] Wessel D, Flugge UI. A method for the quantitative recovery of protein in dilute solution in the presence of detergents and lipids. Anal Biochem 1984;138:141–3.
[12] Balsara BR, Testa JR. Chromosomal imbalances in human lung cancer. Oncogene 2002;21:6877–83.
[13] Björkqvist A-M, Husgafvel-Pursiainen K, Anttila S, Karjalainen A, Tammilehto L, Mattson K, et al. DNA gains in 3q occur frequently in squamous cell carcinoma of the lung, but not in adenocarcinoma. Genes Chromosomes Cancer 1998;22:79–82.
[14] Tisdale MJ. Tumor-host interactions. J Cell Biochem 2004;93:871–7.
[15] Majczak G, Lilla S, Garay-Malpartida M, Markovic J, Medrano FJ, de Nucci G, et al. Prediction and biochemical characterization of intrinsic disorder in the structure of proteolysis-inducing factor/dermcidin. Genet Mol Res 2007;6:1000–11.
[16] Norholm AB, Hendus-Altenburger R, Bjerre G, Kjaergaard M, Pedersen SF, Kragelund BB. The intracellular distal tail of the Na^+/H^+ exchanger NHE1 is intrinsically disordered: implications for NHE1 trafficking. Biochemistry 2011;50:3469–80.
[17] Netea-Maier RT, Hunsucker SW, Hoevenaars BM, Helmke SM, Slootweg PJ, Hermus AR, et al. Discovery and validation of protein abundance differences between follicular thyroid neoplasms. Cancer Res 2008;68:1572–80.
[18] Brown LM, Helmke SM, Hunsucker SW, Netea-Maier RT, Chiang SA, Heinz DE, et al. Quantitative and qualitative differences in protein expression between papillary thyroid carcinoma and normal thyroid tissue. Mol Carcinog 2006;45:613–26.
[19] Katanasaka Y, Ishii T, Asai T, Naitou H, Maeda N, Koizumi F, et al. Cancer antineovascular therapy with liposome drug delivery systems targeted to BiP/GRP78. Int J Cancer/J Int Du Cancer 2010;127:2685–98.
[20] Vedrenne C, Klopfenstein DR, Hauri HP. Phosphorylation controls CLIMP-63-mediated anchoring of the endoplasmic reticulum to microtubules. Mol Biol Cell 2005;16:1928–37.
[21] Wesierska-Gadek J, Gueorguieva M, Kramer MP, Ranftler C, Sarg B, Lindner H. A new, unexpected action of olomoucine, a CDK inhibitor, on normal human cells: up-regulation of CLIMP-63, a cytoskeleton-linking membrane protein. J Cell Biochem 2007;102:1405–19.
[22] Wesierska-Gadek J, Hajek SB, Sarg B, Wandl S, Walzi E, Lindner H. Pleiotropic effects of selective CDK inhibitors on human normal and cancer cells. Biochem Pharmacol 2008;76:1503–14.
[23] Rerole AL, Jego G, Garrido C. Hsp70: anti-apoptotic and tumorigenic protein. Methods Mol Biol 2011;787:205–30.
[24] Garg M, Kanojia D, Seth A, Kumar R, Gupta A, Surolia A, et al. Heat-shock protein 70-2 (HSP70-2) expression in bladder urothelial carcinoma is associated with tumour progression and promotes migration and invasion. Eur J Cancer 2010;46:207–15.
[25] Gastpar R, Gehrmann M, Bausero MA, Asea A, Gross C, Schroeder JA, et al. Heat shock protein 70 surface-positive tumor exosomes stimulate migratory and cytolytic activity of natural killer cells. Cancer Res 2005;65:5238–47.
[26] Li Y, Zhang B, Wang X, Yan H, Chen G, Zhang X. Proteomic analysis of apoptosis induction in human lung cancer cells by recombinant MVL. Amino Acids 2011;41:923–32.
[27] Al-Saad S, Al-Shibli K, Donnem T, Persson M, Bremnes RM, Busund LT. The prognostic impact of NF-kappaB p105, Vimentin, E-cadherin and Par6 expression in epithelial and stromal compartment in non-small-cell lung cancer. Br J Cancer 2008;99:1476–83.
[28] Satelli A, Li S. Vimentin in cancer and its potential as a molecular target for cancer therapy. Cell Mol Life Sci 2011;68:3033–46.
[29] Goldberg Y. Protein phosphatase 2A: who shall regulate the regulator? Biochem Pharmacol 1999;57:321–8.
[30] Ruediger R, Ruiz J, Walter G. Human cancer-associated mutations in the Aalpha subunit of protein phosphatase 2A increase lung cancer incidence in Aalpha knock-in and knockout mice. Mol Cell Biol 2011;31:3832–44.
[31] Ruckova E, Muller P, Nenutil R, Vojtesek B. Alterations of the Hsp70/Hsp90 chaperone and the HOP/CHIP co-chaperone system in cancer. Cell Mol Biol Lett 2012;17:446–58.
[32] Chao A, Lai CH, Tsai CL, Hsueh S, Hsueh C, Lin CY, et al. Tumor stress-induced phosphoprotein1 (STIP1) as a prognostic biomarker in ovarian cancer. PLoS ONE 2013;8:e57084.
[33] Rishi AK, Zhang L, Boyanapalli M, Wali A, Mohammad RM, Yu Y, et al. Identification and characterization of a cell cycle and apoptosis regulatory protein-1 as a novel mediator of apoptosis signaling by retinoid CD437. J Biol Chem 2003;278:33422–35.
[34] Nakata T, Yokota T, Emi M, Minami S. Differential expression of multiple isoforms of the ELKS mRNAs involved in a papillary thyroid carcinoma. Genes, Chromosomes Cancer 2002;35:30–7.
[35] Castets F, Rakitina T, Gaillard S, Moqrich A, Mattei MG, Monneron A. Zinedin, SG2NA, and striatin are calmodulin-binding, WD repeat proteins principally expressed in the brain. J Biol Chem 2000;275:19970–7.
[36] Chen YK, Chen CY, Hu HT, Hsueh YP. CTTNBP2, but not CTTNBP2NL, regulates dendritic spinogenesis and synaptic distribution of the striatin-PP2A complex. Mol Biol Cell 2012;23:4383–92.
[37] Gordon J, Hwang J, Carrier KJ, Jones CA, Kern QL, Moreno CS, et al. Protein phosphatase 2a (PP2A) binds within the oligomerization domain of striatin and regulates the

phosphorylation and activation of the mammalian Ste20-Like kinase Mst3. BMC Biochem 2011;12:54.
[38] Goudreault M, D'Ambrosio LM, Kean MJ, Mullin MJ, Larsen BG, Sanchez A, et al. A PP2A phosphatase high density interaction network identifies a novel striatin-interacting phosphatase and kinase complex linked to the cerebral cavernous malformation 3 (CCM3) protein. Mol Cell Proteom 2009;8:157–71.
[39] Endele S, Fuhry M, Pak SJ, Zabel BU, Winterpacht A. LETM1, a novel gene encoding a putative EF-hand Ca(2^+)-binding protein, flanks the Wolf-Hirschhorn syndrome (WHS) critical region and is deleted in most WHS patients. Genomics 1999;60:218–25.
[40] Fraering PC, Ye W, Strub JM, Dolios G, LaVoie MJ, Ostaszewski BL, et al. Purification and characterization of the human gamma-secretase complex. Biochemistry 2004;43:9774–89.
[41] Gamble SC, Chotai D, Odontiadis M, Dart DA, Brooke GN, Powell SM, et al. Prohibitin, a protein downregulated by androgens, represses androgen receptor activity. Oncogene 2007;26:1757–68.
[42] Dai Y, Ngo D, Jacob J, Forman LW, Faller DV. Prohibitin and the SWI/SNF ATPase subunit BRG1 are required for effective androgen antagonist-mediated transcriptional repression of androgen receptor-regulated genes. Carcinogenesis 2008;29:1725–33.
[43] Bruneel A, Labas V, Mailloux A, Sharma S, Royer N, Vinh J, et al. Proteomics of human umbilical vein endothelial cells applied to etoposide-induced apoptosis. Proteomics 2005;5:3876–84.
[44] Meyer HA, Grau H, Kraft R, Kostka S, Prehn S, Kalies KU, et al. Mammalian Sec61 is associated with Sec62 and Sec63. J Biol Chem 2000;275:14550–7.
[45] Tyedmers J, Lerner M, Bies C, Dudek J, Skowronek MH, Haas IG, et al. Homologs of the yeast Sec complex subunits Sec62p and Sec63p are abundant proteins in dog pancreas microsomes. Proc Natl Acad Sci U S A 2000;97: 7214–9.
[46] Schulmann K, Brasch FE, Kunstmann E, Engel C, Pagenstecher C, Vogelsang H, et al. HNPCC-associated small bowel cancer: clinical and molecular characteristics. Gastroenterology 2005;128:590–9.
[47] Mori Y, Sato F, Selaru FM, Olaru A, Perry K, Kimos MC, et al. Instabilotyping reveals unique mutational spectra in microsatellite-unstable gastric cancers. Cancer Res 2002;62:3641–5.
[48] Klopfenstein DR, Klumperman J, Lustig A, Kammerer RA, Oorschot V, Hauri HP. Subdomain-specific localization of CLIMP-63 (p63) in the endoplasmic reticulum is mediated by its luminal alpha-helical segment. J Cell Biol 2001;153:1287–300.
[49] Nikonov AV, Hauri HP, Lauring B, Kreibich G. Climp-63-mediated binding of microtubules to the ER affects the lateral mobility of translocon complexes. J Cell Sci 2007;120:2248–58.